580.439 Course Notes: Cable Theory

Reading: Koch and Segev, chapt 2, 3, and 5; Johnston and Wu, Chapt. 4. For a detailed treatment of older subjects, see Jack, Noble, and Tsien, 1975. A recent text with up to date discussions of cable theory issues is Koch (1999). Most of the material in these notes is taken from one or another of these texts.

Cable theory was originally applied to the conduction of potentials in an axon by Hodgkin and Rushton (1946) and was later applied to the dendritic trees of neurons by Rall (1962a). The theory itself is much older and was first developed for analyzing underwater telegraph transmission cables. The general problem addressed by cable theory is how potentials spread in a dendritic tree. This is electrotonic conduction and is assumed to occur by passive process, i.e. without action potentials. A typical neuron has thousands of synaptic inputs spread across its surfaces. Cable theory is concerned with how these inputs propagate to the soma or the axon initial segment, how these inputs interact with one another, and how the placement of an input on a dendritic tree affects its functional importance to the neuron.

Derivation of the cable equation

Previously, we have considered only point neuron models. That is, we have assumed that the neuron is electrically compact, so that it can be represented by a single patch of membrane. The gist of this assumption is that the membrane potential is the same everywhere in the neuron. In real neurons, this assumption is not true. Substantial differences in potential exist along the length of a neuron's processes and the resulting longitudinal currents must be explicitly considered.

Figure 1 shows three stages of abstraction of a neuron's dendritic membrane. Figure 1A shows a sketch of the neuron, with its soma at right and a dendrite which branches twice spreading off to the left. One length of membrane cylinder from a secondary branch is isolated in Fig. 1B. It is assumed that the cylinder is of uniform radius along its length (although this assumption can be relaxed, Rall, 1962a). The cylinder is divided into three portions of equal length Δx along the x axis, which runs from left to right. Figure 1C shows an electrical cable model for this length of cylinder. Each of the subcylinders labeled *#1*, *#2*, and *#3* is assumed to be an isopotential patch of membrane. The membrane of each subcylinder is represented by a parallel combination of membrane capacitance $c_m\Delta x$ and an unspecified circuit for the ionic conductances in the membrane, represented by a box. The total current through a membrane patch is $I_m(x)\Delta x$. Note that the membrane current varies with distance x down the cylinder. I_m and c_m are membrane current and capacitance per unit length of cylinder so that multiplying by Δx gives the total current and capacitance in a subcylinder.

The membrane potentials inside the cell $V_i(x)$ and outside the cell $V_e(x)$ are shown at the nodes in Fig. 1C. It is assumed that the potentials also vary with distance down the cylinder, so they are functions of distance x. The membrane potential is $V_i(x)$-$V_e(x)$ as usual. Because the potentials vary along the length of the cylinder, there will be currents $I_i(x)$ and $I_e(x)$ flowing between the nodes. $I_i(x)$ is the total current flowing down the interior of the cylinder and $I_e(x)$ is the total current flowing parallel to the cylinder in the extracellular space. In a real brain there will be many

cylinders from different neurons packed together, so there will be many extracellular currents. $I_e(x)$ is only the portion of the extracullar current associated with the cylinder under study.

The internal current $I_i(x)$ flows through resistance $r_i\Delta x$, which is the resistance of the solutions inside the cylinder between the center of one subcylinder and the center of the next. $r_e\Delta x$

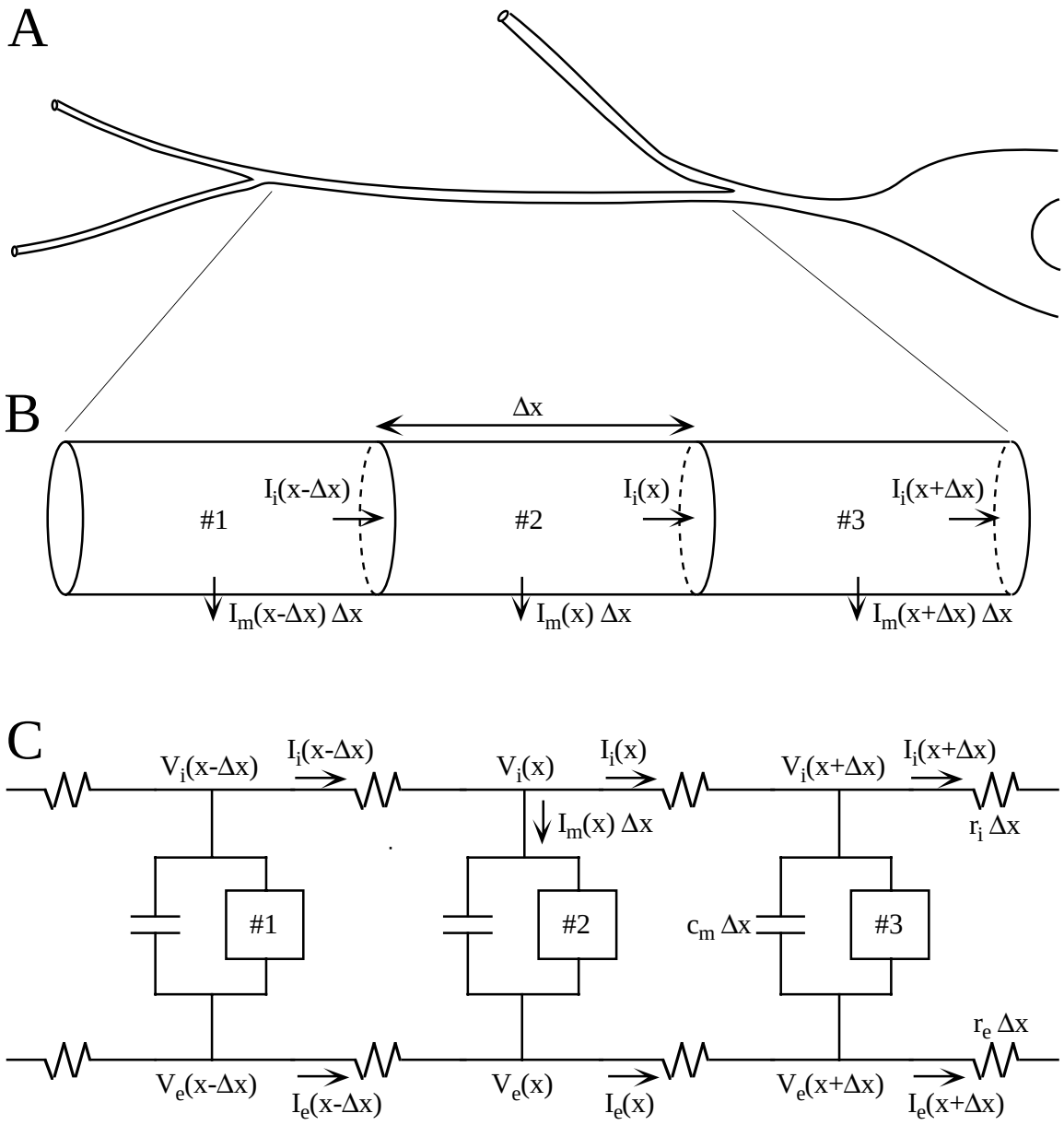

Figure 1. A Sketch of a portion of the dendritic tree of a neuron emerging from the soma at right. B Portion of a secondary dendrite divided into three subcylinders. The axial current I_i and the membrane current I_m are shown next to the arrows. C Discrete electrical model for the three subcylinders. Axial currents flow from one subcylinder to the next through resistances $r_i\Delta x$. Membrane currents flow through a parallel combination of the membrane capacitance $c_m\Delta x$ and membrane ion channels, represented by the boxes. Explicit circuits for the boxes are shown in Fig. 2.

is similarly defined as the resistance in the extracellular space between the center of two subcylinders, i.e. as the resistance to the flow of current $I_e(x)$. r_i and r_e are again defined as resistances per unit length of cylinder.

Ohm's law for current flow in the intracellular and extracellular spaces gives:

$$V_i(x) - V_i(x+\Delta x) = I_i(x)\, r_i\, \Delta x \qquad \text{and} \qquad V_e(x) - V_e(x+\Delta x) = I_e(x)\, r_e\, \Delta x \tag{1}$$

Rearranging and taking the limit as Δx goes to 0,

$$\lim_{\Delta x \to \infty} \frac{V_i(x+\Delta x) - V_i(x)}{\Delta x} = \frac{\partial V_i}{\partial x} = -r_i\, I_i(x) \qquad \text{and} \qquad \frac{\partial V_e}{\partial x} = -r_e\, I_e(x) \tag{2}$$

Conservation of current at the intracellular and extracellular nodes gives

$$\begin{aligned} I_i(x-\Delta x) - I_i(x) &= I_m(x)\, \Delta x \qquad \text{or} \qquad \frac{\partial I_i}{\partial x} = -I_m(x) \\ I_e(x-\Delta x) - I_e(x) &= -I_m(x)\, \Delta x \qquad \text{or} \qquad \frac{\partial I_e}{\partial x} = I_m(x) \end{aligned} \tag{3}$$

Defining the membrane potential as $V = V_i - V_e$ allows the membrane current I_m to be written as the sum of the ionic current $I_{ion}(x,V,t)$ through the box and the current through the membrane capacitance:

$$I_m(x)\, \Delta x = I_{ion}(x,V,t)\, \Delta x + c_m\, \Delta x\, \frac{\partial V}{\partial t} \tag{4}$$

The ionic current is in general a complex and nonlinear function of membrane potential modeled, for example, by Hodgkin-Huxley type equations. As for I_m, I_{ion} is ionic current per unit length of membrane cylinder.

Differentiating and subtracting Eqns. 2 and substituting Eqns. 3 allows the following relationship between membrane potential and membrane current to be written:

$$\begin{aligned} \frac{\partial^2 V}{\partial x^2} &= \frac{\partial^2 (V_i - V_e)}{\partial x^2} \\ &= -r_i \frac{\partial I_i}{\partial x} + r_e \frac{\partial I_e}{\partial x} \\ &= (r_i + r_e)\, I_m \end{aligned} \tag{5}$$

Substituting Eqn. 4 gives the <u>nonlinear cable equation:</u>

$$\frac{1}{r_i + r_e} \frac{\partial^2 V}{\partial x^2} = c_m \frac{\partial V}{\partial t} + I_{ion} \tag{6}$$

Equation 6 models the distribution of membrane potential in a membrane cylinder. The right hand side is the usual equation used for a point neuron model, and expresses the fact that the total membrane current at a point is the sum of the currents through the membrane capacitance and the ion channels. The left hand side is the current injected into the point by the rest of the system, i.e. the current which spreads from adjacent points on the cylinder. The ionic current I_{ion} can be modeled by the usual Hodgkin-Huxley equations.

Equation 6 is linear, but the model for I_{ion} is not, if a full Hodgkin-Huxley model is used. It is useful to consider a simplified, completely linear, version of the cable equation. This is accomplished by using a linear model for I_{ion}. Figure 2 shows circuit diagrams for the membrane

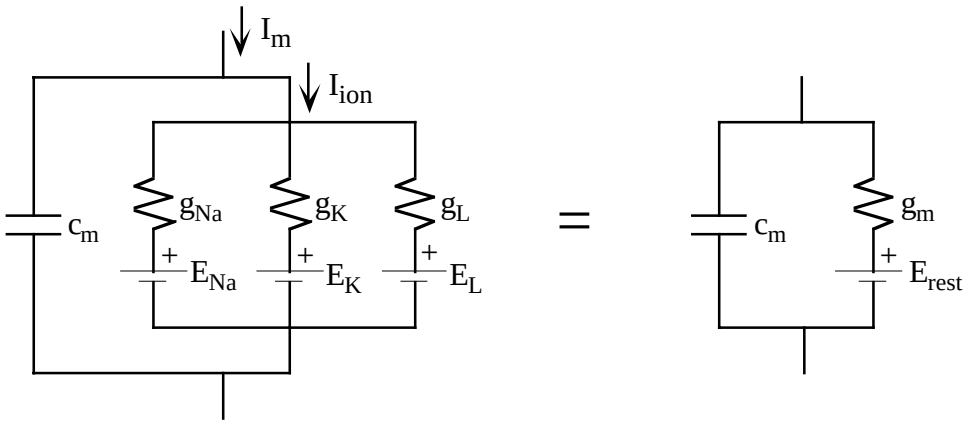

Figure 2 Circuits for the membrane patch. At left is a full Hodgkin-Huxley model, in which g_{Na} and g_K are nonlinear conductances. At right, the resistor-battery circuits have all been combined into a single Thévenin equivalent. In the linear cable model, g_m is assumed to be a constant, linear, conductance.

model, i.e. for the contents of the boxes in Fig. 1. At left is the full model with sodium, potassium, and leakage conductances. In a real neuron, there could be additional parallel battery-resistor combinations for calcium conductances and for multiple kinds of sodium and potassium conductances. In the circuit at right, the battery-resistor pairs have been combined into a single equivalent battery and resistor representing the resting potential E_{rest} and the resting membrane conductance g_m. The single battery-resistor circuit at right is a Thévenin equivalent. See Question 2 for the relationship between the two circuits.

The resistors in the circuit at left in Fig. 2 are non-linear and the membrane conductance g_m in the circuit at right is also non-linear, in the absence of further assumptions. To derive a linear cable equation, it will be assumed that g_m is a constant, linear resistance equal to the resting conductance of the membrane. This is an approximation which is valid only to the extent that membrane potential excursions are small enough not to induce significant gating of the voltage-dependent channels in the real membrane circuit. Given recent evidence, it is clear that dendritic trees contain significant densities of voltage-gated channels and that these channels participate in the responses to synaptic activation. Nevertheless, there are many insights into the functioning of dendritic trees that can only be gained from analysis of the linear cable model.

If g_m is a linear resistance, then $I_{ion}=g_m(V-E_{rest})$. Substituting this in Eqn. 6 and changing the membrane potential variable to $v=V-E_{rest}$, gives the linear cable equation.

$$\frac{1}{r_i + r_e}\frac{\partial^2 v}{\partial x^2} = c_m \frac{\partial v}{\partial t} + g_m v = c_m \frac{\partial v}{\partial t} + \frac{1}{r_m} v \tag{7}$$

where use has been made of the fact that, because E_{rest} is a constant

$$\begin{gathered} \partial^2 V / \partial x^2 = \partial^2 (V - E_{rest}) / \partial x^2 = \partial^2 v / \partial x^2 \\ \text{and} \\ \partial V / \partial t = \partial (V - E_{rest}) / \partial t = \partial v / \partial t \end{gathered} \tag{8}$$

Equation 7 can be rewritten in a non-dimensional form by multiplying both sides by membrane resistance r_m

$$\frac{r_m}{r_i + r_e}\frac{\partial^2 v}{\partial x^2} = r_m c_m \frac{\partial v}{\partial t} + v \qquad \text{or} \qquad \lambda^2 \frac{\partial^2 v}{\partial x^2} = \tau_m \frac{\partial v}{\partial t} + v \tag{9}$$

Two new constants are defined here, the length constant λ and the membrane time constant τ_m. These names will be justified in terms of the solutions derived in later sections. Now define new dimensionless distance and time variables χ and T as $\chi = x / \lambda$ and $T = t / \tau_m$. Finally, the linear cable equation can be written in terms of the dimensionless variables as

$$\frac{\partial^2 v}{\partial \chi^2} = \frac{\partial v}{\partial T} + v \tag{10}$$

which follows from the chain rule for derivatives. Equation 10 is the form in which the cable equation will be used for most of the rest of the discussion.

Question 1. Show that $\partial V_e^2 / \partial x^2 = -r_e I_m$. Under appropriate conditions, this equation can be used to infer membrane current density I_m from extracellular potential measurements V_e only. What anatomical features of the system are necessary to allow this calculation? Hint: the equation is one-dimensional; under what conditions is the extracellular potential near a group of neurons likely to vary along one axis only? Describe how the calculation would be done.

Question 2. Show that, for the circuits in Fig. 2:

$$E_{rest} = \frac{g_{Na} E_{Na} + g_K E_K + g_L E_L}{g_{Na} + g_K + g_L} \qquad \text{and} \qquad \mathrm{g_m} = g_{Na} + g_K + g_L \tag{11}$$

Question 3. Consider the case in which the membrane consists only of a leakage channel and a Hodgkin-Huxley type delayed rectifier potassium channel (left side of Fig. 3). It was shown in class and on a homework that this nonlinear circuit can be approximated by the linear circuit at right in Fig. 3; the approximation is accurate if membrane potential excursions from the resting potential are small. Derive a linear cable equation for this small-signal equivalent model for the membrane patch. Note that it will not be possible to write this as a single equation in the form of Eqn. 7; instead two linear differential equations will be required. However if the system is Laplace or Fourier transformed, then a single equation of the form $d^2 \overline{V} / dx^2 = A \overline{V}$ can be derived. A is a

complex scalar function of the Fourier or Laplace transform variable and $\overline{V}$ is the Fourier or Laplace transformed membrane potential. Derive an expression for *A* in terms of the parameters of the linear circuit in Fig. 3.

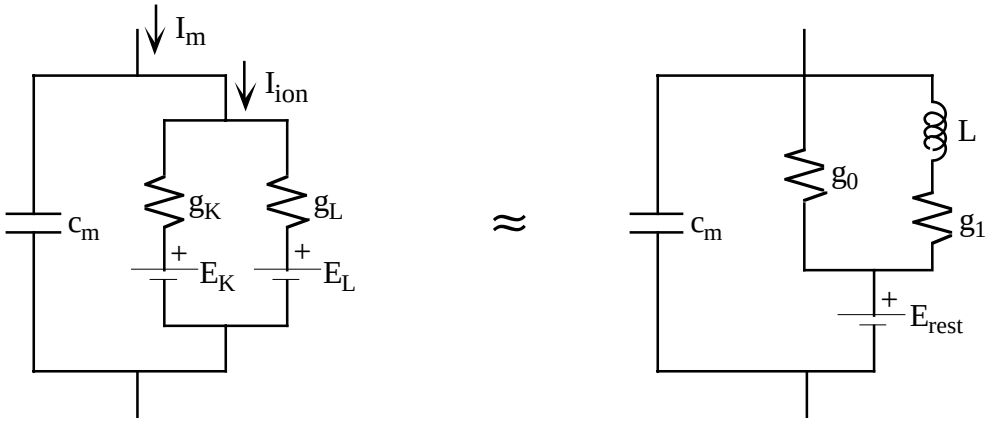

Figure 3 At left is a circuit patch model for a membrane containing only a leakage channel g_L and a Hodgkin-Huxley type delayed rectifier channel g_K. At right is a linear approximation of the nonlinear circuit.

Cable equation parameters

The parameters of the cable model are defined in this section. Various electrical parameters of neural cables are introduced and defined. For all the following, *a* is the radius of the membrane cylinder.

r_i = resistance of the solution inside a unit length of membrane cylinder to axial current flow I_i, with units like Ω/cm.

= $R_i / \pi a^2$ where R_i is the resistivity of the solution, defined as the resistance from one face to the opposite face for a cube of solution of unit dimensions. Typically R_i is 60-200 Ω·cm for neural cytoplasm. r_i is equal to the resistance of a unit length of cylinder of cross sectional area πa^2.

c_m = capacitance of the membrane of a unit length of membrane cylinder, with units like μFd/cm.

= $2\pi a C$ where C is the capacitance of a unit area of membrane. For neurons, $C \approx 1$ μFd/cm^2. c_m is the capacitance of a unit length of cylinder with radius *a*, which therefore has surface area $2\pi a$.

$g_m = 1/r_m$ = conductance of the membrane of a unit length of membrane cylinder, with units like S/cm. Note that the resistance of a unit length, r_m has units Ω·cm.

= $2\pi a / R_m$ where R_m is the resistance of a unit area of membrane. For neurons, R_m is generally in the range $10^4 - 10^5$ Ω·cm^2. It would be more intuitive to express R_m as a conductance with units S/cm^2 by analogy to *C*. However, in virtually all publications, this constant is given in terms of resistance. g_m or $1/r_m$ is the conductance of a unit length of cylinder with surface area $2\pi a$.

r_e = resistance to longitudinal flow of current in the extracellular space, with units like Ω/cm. This constant is not defined in terms of the parameters of the membrane cylinder. Instead, it is assumed to be negligible compared to the other impedances in the circuit and ignored, i.e. r_e = 0.

Given the parameters defined above, the length constant and membrane time constants can be specified in terms of more fundamental parameters. These are given below along with a new constant G_∞ which is the input conductance of an semi-infinite cylinder. The properties of G_∞ will be derived in a later section.

λ = length constant, with units cm. From Eqn. 9,

$$= \sqrt{\frac{r_m}{r_e + r_i}} \approx \sqrt{\frac{r_m}{r_i}} = \sqrt{\frac{R_m\, a}{2\, R_i}} \qquad (12)$$

where the assumption $r_e << r_i$ has been used to eliminate r_e from the equation. Note that λ varies as the square root of cylinder radius a.

τ_m = membrane time constant. Also from Eqn. 9,

$= r_m c_m = R_m C$

Note that τ_m does not depend on cylinder radius.

G_∞ = input conductance of a semi-infinite cylinder at its end.

$$= \frac{1}{r_i \lambda} = \sqrt{\frac{2}{R_i\, R_m}}\, \pi a^{3/2} \qquad (13)$$

The dependence of G_∞ on the 3/2 power of cylinder radius will be important in considering the equivalent cylinder theorem in a later section.

Solutions for a semi-infinite cylinder

The basic properties of electrotonic conduction can be seen by considering a simple case, a semi-infinite cylinder driven with a step of current at its end. The cylinder is shown in Fig. 4 . The step of current is injected at the end of the cylinder (x=χ=0) and we want to know the time course of membrane potential in the cylinder at various positions.

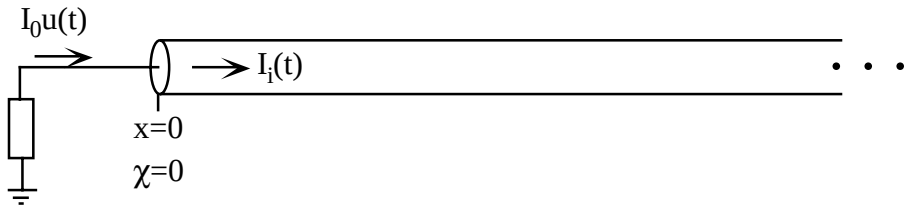

Figure 4. Semi-infinite cable driven by a step current at its end.

The problem to be solved is the cable equation, Eqn. 10, with suitable boundary conditions. The cable equation needs one boundary condition in the time domain and two in the spatial domain. For almost all cable theory problems, the appropriate time boundary condition is a zero initial condition, i.e. $v(\chi,T=0) = 0$. One spatial boundary condition for this case is that the axial current in the cable must equal the external current injected. Using Eqn. 2 and assuming that $r_e=0$ so that V_e can be ignored, the boundary condition can be written in terms of membrane potential as

$$I_0\, u(T) = I_i(\chi = 0, T)$$

$$= -\frac{1}{r_i}\frac{\partial v}{\partial x}\bigg|_{x=0} = -\frac{1}{r_i \lambda}\frac{\partial v}{\partial \chi}\bigg|_{\chi=0} = -G_\infty \frac{\partial v}{\partial \chi}\bigg|_{\chi=0} \tag{14}$$

Note that v, the membrane potential relative to rest, has been substituted for V, the absolute membrane potential, as justified by Eqn. 8. Eqn. 14 provides one boundary condition in space. For this problem, a second boundary condition cannot be given, but the condition that the membrane potential must remain finite over the whole cable (a regularity condition) will suffice as a second constraint.

The problem to be solved is as follows:

$$\frac{\partial^2 v}{\partial \chi^2} = \frac{\partial v}{\partial T} + v$$

$$v(\chi, T = 0) = 0 \tag{15}$$

$$\frac{\partial v}{\partial \chi}\bigg|_{\chi=0} = -\frac{I_0}{G_\infty} u(t) \quad \text{and} \quad v(\chi, T) < \infty \text{ for all } \chi, T$$

A convenient way to solve problems of this kind is to Laplace transform the variables over the time domain. The Laplace transform of a time function $v(t)$ is defined as follows:

$$\bar{V}(s) = \mathbf{L}[v(t)] = \int_0^\infty v(t) e^{-st}\, dt \tag{16}$$

where $\bar{V}(s)$ is the transformed function and s is the transform variable. Laplace transforms are useful because of the following property:

$$\mathbf{L}[dv/dt] = s\bar{V} - v(t = 0) \tag{17}$$

With this property, differential equations are reduced to algebraic equations, which often simplifies solving the equations.

Transforming the cable equation problem of Eqn. 15 along with its boundary conditions gives

$$\frac{\partial^2 \overline{V}}{\partial \chi^2} = (s+1)\,\overline{V}$$
$$\left.\frac{\partial \overline{V}}{\partial \chi}\right|_{\chi=0} = -\frac{I_0}{s\,G_\infty} \quad \text{and} \quad v(\chi,T) < \infty \text{ for all } \chi, T \tag{18}$$

The membrane potential variable $v(\chi,T)$ has been replaced with the transformed variable $\overline{V}(\chi,s)$. Because Laplace transformation and differentiation are both linear operations, the Laplace transformation does not affect the derivatives with respect to χ in Eqn. 18. The time derivative has been replaced with a multiplication by s as in Eqn. 17 and the zero initial condition has been used as part of that operation. The spatial boundary condition at 0 was transformed, using the fact that $\mathbf{L}[u(t)] = 1/s$. The spatial regularity condition of finite v cannot be transformed directly, but will be used below.

Equation 18 is now an ordinary differential equation whose solution takes the form

$$\overline{V}(\chi,s) = A(s)e^{\sqrt{s+1}\chi} + B(s)e^{-\sqrt{s+1}\chi} \tag{19}$$

where $A(s)$ and $B(s)$ are to be determined from the boundary conditions. Using the boundary condition at 0,

$$\begin{aligned}\left.\frac{\partial \overline{V}}{\partial \chi}\right|_{\chi=0} &= \left[\sqrt{s+1}\;A(s)\,e^{\sqrt{s+1}\chi} - \sqrt{s+1}\;B(s)\,e^{-\sqrt{s+1}\chi}\right]\Big|_{\chi=0} \\ &= \sqrt{s+1}\,[A(s) - B(s)] = -\frac{I_0}{s\,G_\infty}\end{aligned} \tag{20}$$

The additional condition needed to uniquely specify A and B is the regularity condition. From experience with exponential solutions like Eqn. 19, it seems likely that either A or B should be zero so that as $\chi \to \infty$, the membrane potential remains finite. However, the solution in Eqn. 19 is in terms of the Laplace transform and it is not clear how to directly apply this condition. To apply the regularity condition, assume that $B(s)$=0; in that case Eqns. 19 and 20 give the following solution:

$$\overline{V}(\chi,s) = -\frac{I_0}{G_\infty}\,\frac{e^{\sqrt{s+1}\chi}}{s\sqrt{s+1}} \tag{21}$$

The regularity condition must hold in all conditions, including in the steady state as $T \to \infty$. This so-called final value can be computed from a theorem of Laplace transforms:

$$\lim_{t \to \infty} v(t) = \lim_{s \to 0} s\overline{V}(s) \tag{22}$$

Applying the final value theorem to Eqn. 21 gives $v(\chi, T \to \infty) = -I_0\, e^{\chi} / G_\infty$. Clearly this function does not remain finite as χ goes to infinity. Thus we must conclude that $A(s)$=0 and the solution for the Laplace transform of membrane potential is

$$\overline{V}(\chi,s)=\frac{I_0}{G_\infty}\,\frac{e^{-\sqrt{s+1}\,\chi}}{s\sqrt{s+1}} \tag{23}$$

The membrane potential function can now be obtained by inverting the Laplace transform in Eqn. 23. The method for accomplishing this is described in Jack et al. (1975, chapter 3) and in Hodgkin and Rushton (1946). The solution is as follows:

$$v(\chi,T)=\frac{I_0}{2G_\infty}\left\{e^{-\chi}\ \mathrm{erfc}\left[\frac{\chi}{2\sqrt{T}}-\sqrt{T}\right]-e^{\chi}\ \mathrm{erfc}\left[\frac{\chi}{2\sqrt{T}}+\sqrt{T}\right]\right\} \tag{24}$$

The function erfc(x) is the complementary error function, defined as

$$erfc(x)=1-\frac{2}{\sqrt{\pi}}\int_0^x e^{-\xi^2}\,d\xi \tag{25}$$

Figure 5A shows plots of exp(-x^2**)** and erfc(x) for reference; erfc is a standard function and algorithms for computing it are found in Matlab and other mathematics programs.

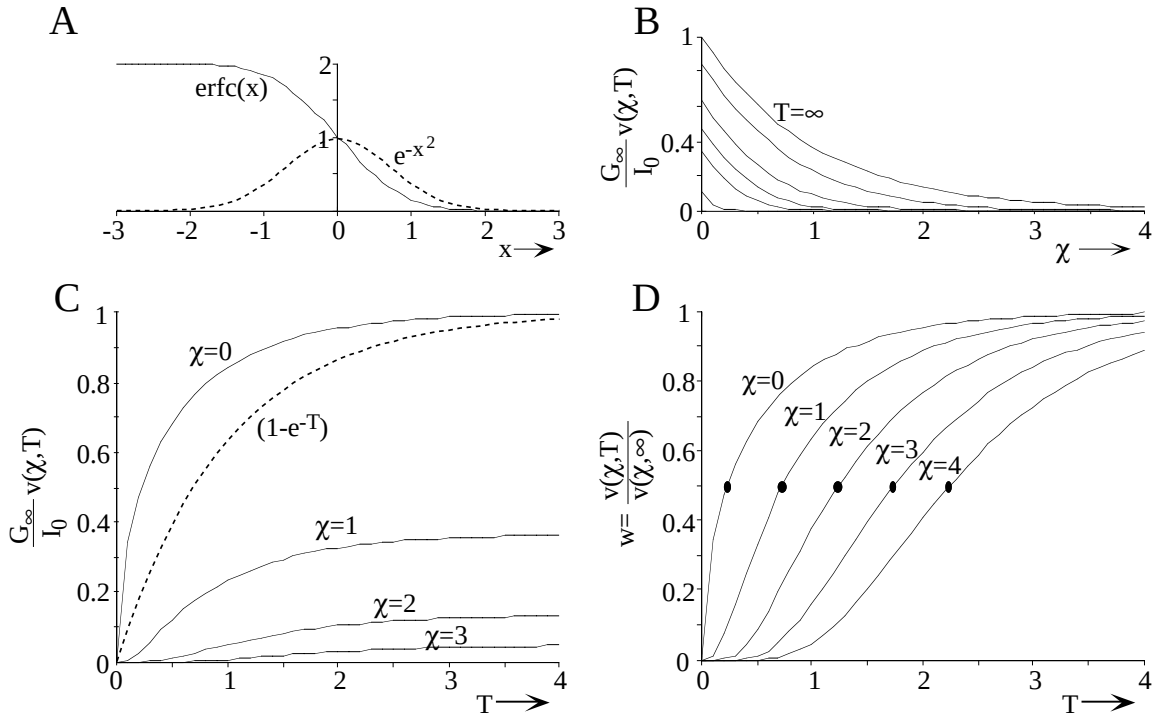

Figure 5. A. Plots of exp(-x^2) and erfc(x). B. Plot of the distribution of the membrane potential along the cylinder (Eqn. 24) at 6 times: T=0.01, 0.1, 0.2, 0.4, 1.0, and ∞. Membrane potential is normalized by its steady state value at χ=0 (I_0/G_∞). C. Plot of the time course of membrane potential at four locations along the cylinder, normalized as in B. For comparison, an exponential rise is also plotted. D. Same as C except membrane potential is normalized by its steady state value.

Several important properties of the solutions to the cable equation can be seen from plots of Eqn. 24 in Fig. 5.

1. Figure 5C shows plots of the growth of membrane potential in response to the step current injection; each curve shows potential growth at a different position along the cylinder, as labeled. Note that at χ=0 the potential grows to a steady value relatively quickly. The growth is faster than exponential, as seen by the comparison with the function (1-exp(-*T*)), which is plotted for comparison. As the point moves away from the end of the cable (larger χ), the growth of potential is delayed and the steady state value of potential is smaller. The difference in growth rate can be seen in Fig. 5D where the same plots are shown, except normalized by their maximum value. Note that the membrane time constant τ_m sets the time scale of the response, in that the abscissae of Figs. 5C and 5D are scaled in units of τ_m.

   Figure 5C illustrates the basic features of electrotonic conduction: as the potential spreads from the site of a disturbance (in this case the current injection at the end of the cable), the amplitude of the potential gets smaller and its time course is extended. In this case, the rise of the potential is delayed and its rise is slower.

2. Figure 5B shows the potential spread along the cylinder at various times following the onset of the current at *T*=0. The most illuminating case is for *T*=∞, i.e. in the steady state. In the steady state, Eqn. 24 becomes

$$v(\chi, T \to \infty) = \frac{I_0}{G_\infty} e^{-\chi} = \frac{I_0}{G_\infty} e^{-x/\lambda} \tag{26}$$

   This equation illustrates the meaning of the space constant λ. The decay of potential is exponential along the cylinder, so that potential decays by 1/e for every distance λ. Thus the space constant is a measure of how far a disturbance spreads away from the point of current injection.

   Equation 26 also allows the meaning of the parameter G_∞ to be understood. Note that at χ=0, $v(T=\infty)=I_0/G_\infty$. Thus the resistance looking into the end of the semi-infinite cylinder in the steady state, for application of D.C. current, is $1/G_\infty$. This is the basis for the statement made earlier that G_∞ is the input conductance of a semi-infinite cable.

3. A measure of the speed of electrotonic spread can be gotten from the points marked by black circles in Fig. 5D. These circles mark the times at which the potential is half its steady state value, for different values of χ. If the χ values are plotted against the half-times, the result is a straight line with slope $2\lambda/\tau_m$ (Jack et al., 1975). This value can be though of as the speed of spread of electrotonic disturbances. Of course, it is not a true propagation speed, in the sense of the action potential propagation speed, because there is no fixed waveshape that is propagating, i.e. this is not a true wave. Nevertheless, this speed provides a way to calculate the time delays expected in electrotonic conduction. Note that it varies as the square root of the cylinder radius, since

$$\text{speed} = 2\frac{\lambda}{\tau_m} = \sqrt{\frac{2\,a}{R_m\,R_i\,C^2}} \tag{27}$$

Question 4 Suppose that the current injected into the semi-infinite cable in Fig. 4 is an impulse, $Q_0\delta(t)$. Solve for the potential distribution in the cable as a function of time and χ. The following Laplace transform pair will be helpful:

$$\frac{e^{-x\sqrt{s}}}{\sqrt{s}} \leftrightarrow \frac{e^{-x^2/4t}}{\sqrt{\pi t}}$$

It will also be helpful to know the frequency shift property: $\mathbf{L}\left[e^{-at} f(t)\right] = \overline{F}(s+a)$. This was one model that was considered for neurons in early papers. The idea was that the dendritic tree is very long, so it could be approximated as infinite, and the soma was unimportant. Show that the membrane time constant τ_m can be determined from a plot of $\ln\left[\sqrt{t}\ v(0,t)\right]$ versus t.

The Rall motorneuron model

This model is diagrammed in Fig. 6 and provides a good framework for discussing other boundary conditions for the cable equation. The model contains a soma, represented by the passive elements C_S and G_S which are the somatic capacitance and resting conductance. Note the assumption that the soma is isopotential, so that it can be represented by a single point model of this type. Of course, active conductances in the soma and axon are ignored in this model. The dendritic tree is represented by a single cable of physical length x_l and electrotonic length x_l/λ. In a later section, the matter of representing a whole dendritic tree as a single cylinder will be discussed in more detail. Under certain assumptions, this turns out to be a good approximation. Also shown is a current $I_0u(t)$ which is injected into the soma from an external electrode.

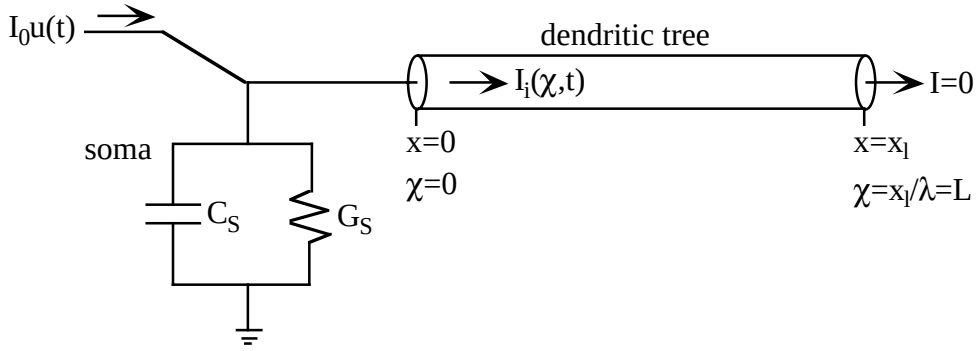

Figure 6. Rall motorneuron model. The soma is represented by the point-model consisting of the somatic capacitance C_S and resting conductance G_S. The dendritic tree is represented by a single membrane equivalent cylinder, which runs from x=0 to x=x_l. L is the electrotonic length of the dendritic cable. $I_0u(t)$ is an external current injected into the soma of the cell through a microelectrode.

At the right end of the cable, it is assumed that there is zero axial current. This boundary condition is frequently assumed for the end of the dendritic tree. The idea is that the dendrites taper down to a point and so no axial current flows at the tips. This zero-current boundary condition means that

$$\left.\frac{\partial v}{\partial \chi}\right|_{\chi=L} = 0 \tag{28}$$

At the soma, the boundary condition involves balance of the four currents involved: the external injected current, the current through the somatic capacitance, the current through the somatic resistance, and the current into the cable. Also it is assumed that the somatic membrane potential is equal to $v(\chi=0,T)$, i.e. that the membrane potential at the soma is the same as the membrane potential at the soma end of the cable. Using the same method as for Eqn. 14 gives

$$\begin{aligned} I_0\, u(t) &= C_S \left.\frac{\partial v}{\partial t}\right|_{\chi=0} + G_S\, v(\chi=0,T) - G_\infty \left.\frac{\partial v}{\partial \chi}\right|_{\chi=0} \\ &= \frac{C_S}{\tau_m} \left.\frac{\partial v}{\partial T}\right|_{\chi=0} + G_S\, v(\chi=0,T) - G_\infty \left.\frac{\partial v}{\partial \chi}\right|_{\chi=0} \end{aligned} \tag{29}$$

Note the handling of the time variables t and T in the term for capacitive current in the soma.

Question 5 The cable equation model for the Rall motorneuron is usually solved using separation of variables techniques (Rall, 1969). However, it can also be solved with the Laplace transform methods described above, if the boundary condition at $\chi=L$ is thrown away. Suppose the dendritic cable is infinitely long, as in Fig. 4. Solve the cable equation to derive the Laplace transform of the membrane potential in the dendritic tree for the situation in Fig. 6, except for the infinite cable assumption. Express your solution in terms of two new parameters, $\rho=G_\infty/G_S$ the dendritic dominance and $\varepsilon=C_S/(\tau_m G_S)$.

Cable equation in finite cylinders

To reconstruct an arbitrary dendritic tree, it is necessary to have a general solution for the membrane potential in a finite cylinder and a way to handle arbitrary boundary conditions like those in Eqn. 29. The basis for this is the two-port model drawn in Fig. 7. The cable has electrotonic length L. At its two ends there are current and membrane potential boundary conditions as shown. What these mean is that

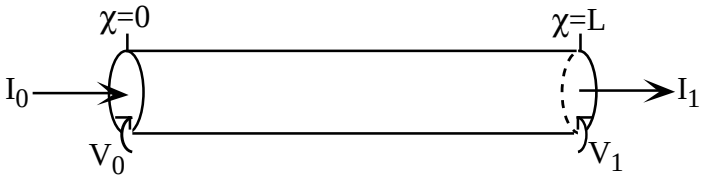

Figure 7. Two-port model for a length of dendritic cylinder

$$\begin{aligned} v(\chi=0,T) &= V_0(T) \quad \text{and} \quad v(\chi=L,T) = V_1(T) \\ I_i(\chi=0,T) &= I_0(T) \quad \text{and} \quad I_i(\chi=L,T) = I_1(T) \end{aligned} \tag{30}$$

The components of Eqn. 30 serve as boundary conditions for the cable equation in the cylinder of Fig. 7. Of course, a cable problem can have only two boundary conditions in the spatial dimension,

so two of the equations in Eqn. 30 are boundary conditions which can be freely specified and the other two are fixed once the first two are chosen. In general, any two of the four can be chosen as boundary conditions.

There must also be a boundary condition in the time dimension. One of three situations will be considered. In each case, the cable equation is reduced to the ordinary differential equation

$$\frac{d^2\overline{V}}{d\chi^2} = q^2\overline{V} \tag{31}$$

where q is a variable that depends on the situation considered. The three situations are as follows:

1. D.C. steady state: in this case, all the sources are D.C. values and enough time has elapsed that the membrane potential and all currents in the system are steady, not varying with time. In this case $\partial v/\partial T = 0$ in Eqn. 10, q=1, and $\overline{V} = v$ in Eqn. 31.

2. Laplace transform from zero initial conditions: this is the same transform that was applied in Eqns. 15-18. In this case, $q = \sqrt{s+1}$ and $\overline{V}(\chi, s)$ is the Laplace transform of $v(\chi,T)$. The boundary conditions are also Laplace transformed.

3. Fourier transform in the sinusoidal steady state: this is similar to case 2. The sources are all sinusoidal at frequency ω and have been applied to the system long enough that transient components have died away. In this steady state, the membrane potentials and currents are also sinusoidal at frequency ω. Then, $q = \sqrt{1+j\omega}$, where $j = \sqrt{-1}$, and $\overline{V}(\chi, j\omega)$ is the Fourier transform of $v(\chi,T)$. The boundary conditions are also Fourier transformed in this case.

Below, Eqn. 31 will be used as the cable equation; the equation will be solved for the situation diagrammed in Fig. 7, where the voltages and currents shown in the figure are transformed in the same way as the cable equation. That is, if situation 1 applies, then V_0, V_1, I_0, and I_1 are D.C. values also. If situation 2 applies, then these signals are the Laplace transforms of the boundary voltages and currents.

The solution to Eqn. 31 can be written as

$$\overline{V}(\chi, q) = A(q)\sinh(q\chi) + B(q)\cosh(q\chi) \tag{32}$$

where sinh(x)=[exp(x)-exp(-x)]/2 and cosh(x)=[exp(x)+exp(-x)]/2. It will also be useful to have the axial current $\bar{I}_i(\chi, q) = -G_\infty\, \partial\overline{V}/\partial\chi$ (from Eqn. 14); from Eqn. 32, this is

$$\bar{I}_i(\chi, q) = -G_\infty\, q\left[A(q)\cosh(q\chi) + B(q)\sinh(q\chi)\right] \tag{33}$$

The constants $A(q)$ and $B(q)$ must determined from the boundary conditions of Fig. 7 and Eqn. 30. As was discussed above, only two of the possible boundary conditions can be applied at once. One useful result can be derived by choosing to specify V_0 and I_0. This gives the following boundary conditions, using Eqns. 32 and 33:

$$\bar{V}(0,q) = B = \bar{V}_0 \quad \text{and} \quad \bar{I}_i(0,q) = -G_\infty q A = \bar{I}_0 \tag{34}$$

A and *B* are determined by Eqn. 34, resulting in the following solution for membrane potential and axial current in the finite cable.

$$\begin{bmatrix} \bar{V}(\chi,q) \\ \\ \bar{I}_i(\chi,q) \end{bmatrix} = \begin{bmatrix} \cosh(q\chi) & -\sinh(q\chi)/G_\infty q \\ \\ -G_\infty q \sinh(q\chi) & \cosh(q\chi) \end{bmatrix} \begin{bmatrix} \bar{V}_0 \\ \\ \bar{I}_0 \end{bmatrix} \tag{35}$$

Note that $\bar{V}_1$ and $\bar{I}_1$ are specified in this case by the functions in Eqn. 35 evaluated at χ=*L*.

A second useful solution begins with an alternative way of writing the solutions to the cable equation, Eqn. 31:

$$\begin{aligned} \bar{V}(\chi,q) &= A(q)\sinh[q(L-\chi)] + B(q)\cosh[q(L-\chi)] \\ \bar{I}_i(\chi,q) &= G_\infty q\left\{A(q)\cosh[q(L-\chi)] + B(q)\sinh[q(L-\chi)]\right\} \end{aligned} \tag{36}$$

In this case, applying the boundary conditions at χ=*L*, i.e. $\bar{V}_1$ and $\bar{I}_1$ gives

$$\begin{bmatrix} \bar{V}(\chi,q) \\ \\ \bar{I}_i(\chi,q) \end{bmatrix} = \begin{bmatrix} \cosh[q(L-\chi)] & \sinh[q(L-\chi)]/G_\infty q \\ \\ G_\infty q \sinh[q(L-\chi)] & \cosh[q(L-\chi)] \end{bmatrix} \begin{bmatrix} \bar{V}_1 \\ \\ \bar{I}_1 \end{bmatrix} \tag{37}$$

Many other versions of Eqns. 35 and 37 can be derived by considering various combinations of boundary conditions. However, these two equations are sufficient to allow derivation of the equations needed to analyze finite cables and arbitrarily shaped dendritic trees. An example which leads to an important results for finite cables is the situation diagrammed in Fig. 8. It is assumed that the cable is loaded at its right hand end with an admittance Y_L. Y_L is transformed in the same way as the voltage and current variables; that is, if the cable is in the D.C. steady state (situation 1 above), the Y_L is the conductance of the load; if the cable equation was Laplace transformed from 0 initial conditions, then Y_L is the inverse of the complex impedance of the load. The load applies one constraint to the problem of the form $\bar{I}_1 = Y_L \bar{V}_1$. The second constraint is to assume that the voltage $\bar{V}_0$ is known, for example because of a voltage clamp at χ=0. Substituting the constraint provided by the load into Eqn. 37 gives the following two equations:

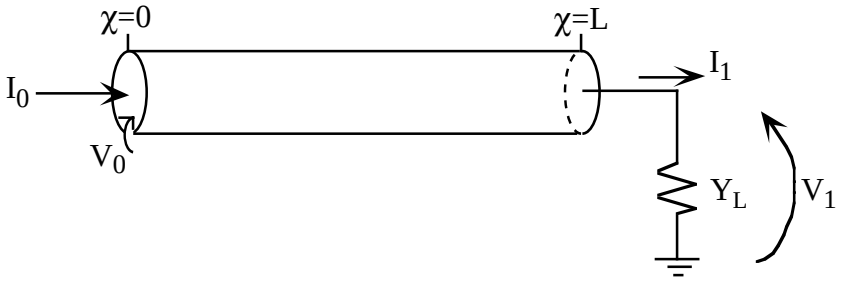

Figure 8. Finite cable loaded with an admittance Y_L at one end and voltage clamped at the other.

$$\begin{bmatrix} \bar{V}(\chi,q) \\ \\ \bar{I}_i(\chi,q) \end{bmatrix} = \begin{bmatrix} \cosh[q(L-\chi)] & \sinh[q(L-\chi)]/G_\infty q \\ \\ G_\infty\, q \sinh[q(L-\chi)] & \cosh[q(L-\chi)] \end{bmatrix} \begin{bmatrix} \bar{V}_1 \\ \\ Y_L\, \bar{V}_1 \end{bmatrix} \tag{38}$$

The constraint that $\bar{V}(\chi=0,q)=\bar{V}_0$ can be applied to solve for $\bar{V}_1$, the one unknown in Eqn. 38. Using the voltage equation in Eqn. 38 gives

$$\bar{V}_0 = \bar{V}(\chi=0,q) = \bar{V}_1\left(\cosh qL + \frac{Y_L}{G_\infty q}\sinh qL\right) \tag{39}$$

Using Eqn. 39 to eliminate $\bar{V}_1$ in Eqn. 38 gives the membrane potential in this finite cylinder as

$$\bar{V}(\chi,q) = \bar{V}_0 \frac{\cosh[q(L-\chi)] + \dfrac{Y_L}{G_\infty q}\sinh[q(L-\chi)]}{\cosh qL + \dfrac{Y_L}{G_\infty q}\sinh qL} \tag{40}$$

Figure 9 shows plots of Eqn. 40 for the D.C. steady state situation (q =1). In this semilogarithmic plot, the potential decay would be a straight line for the exponential decay of the infinite cylinder model (Eqns. 24 and 26). Figure 9 shows the effect of the load impedance on the spread of potential in a finite cylinder. When Y_L/G_∞=1, the decay is a straight line and is exactly what would occur in an infinite cylinder. For smaller loads ($Y_L<G_\infty$), the potential in the finite cylinder decays more slowly and for larger loads, it decays more rapidly.

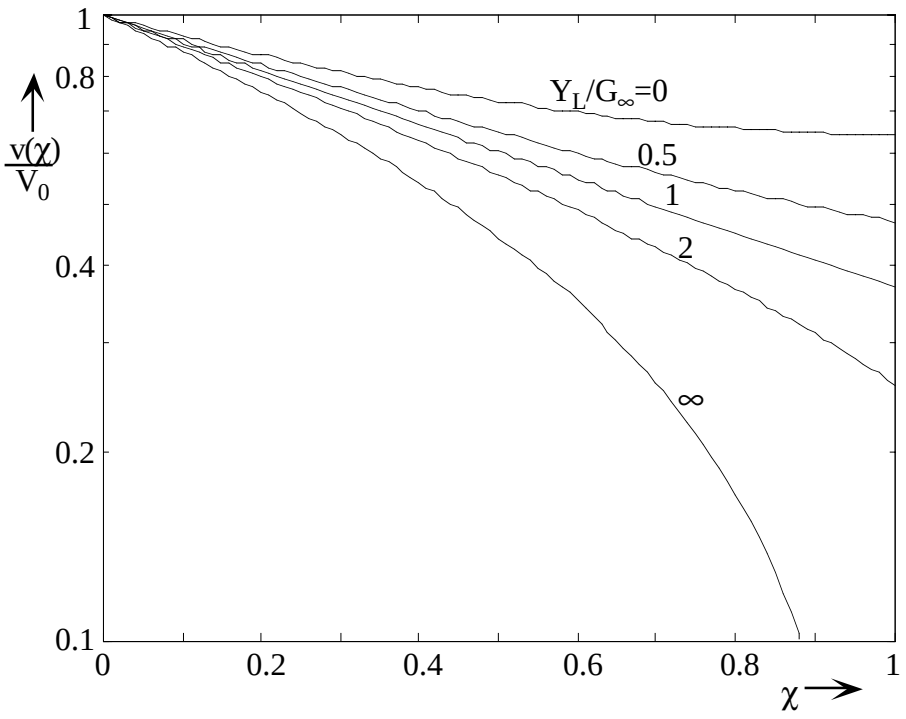

Figure 9 Decay of potential in a finite cylinder of electrotonic length 1 for the D.C. steady state case. Cylinder is voltage clamped at one end and terminated by a load admittance Y_L at the other (Fig. 8). Parameters on the curves are load admittance values relative to G_∞.

The transfer impedance approach to dendritic trees

This approach to dendritic trees is designed to answer questions about the relationships of signals in different parts of the tree. For example, several points are marked on the dendritic tree in

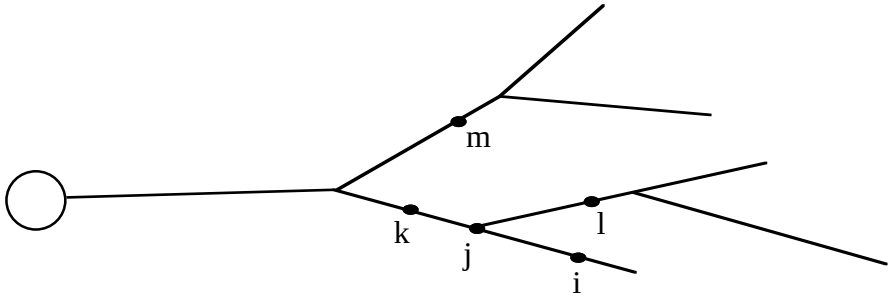

Figure 10 Example of a branching dendritic tree with several points marked for the discussion of transfer impedance.

Fig. 10. The questions of interest concern the interrelationships of the signals at these points. For example, if a current is injected at point *i*, what is the potential at the other points? How closely linked are these points in electrical terms, i.e. how much do potentials at one point influence the others? How do currents injected at these points affect the others?

In order to answer questions of this type, it turns out to be sufficient to use three rules. These are developed below and then applied in some examples. Please note that these rules are effective for linear problems only. This means problems in which the input is a current or a voltage and the output is a current or voltage. It excludes problems in which the input is a conductance change, as is appropriate for synapses. The issue of linearity and non-linearity of synapses is discussed in a later section.

Rule 1: voltage transfer ratio This situation has already been analyzed. It is diagrammed in Fig. 8. What is desired is the voltage gain from V_0 to V_1 in the presence of a load admittance Y_L. From Eqn. 39,

$$A_{01} = \frac{\overline{V}_1}{\overline{V}_0} = \frac{1}{\cosh qL + \frac{Y_L}{G_\infty q}\sinh qL} \tag{40}$$

The gain A_{01} is transformed in the same way as the voltages and currents. That is, if the situation is the D.C. steady state, then A_{01} is the D.C. voltage ratio, a real number; if the cable equation has been Laplace transformed from 0 initial conditions, then A_{01} is the complex transfer gain, a function of *s*.

This rule expresses the spread of voltage in the tree. For example, in Fig. 10, if $\overline{V}_i$ is known, then $\overline{V}_j$, $\overline{V}_k$, etc.can be computed by application of Eqn. 40 (assuming that Y_L can be computed, the method for doing this is described below) either once or several times. Note that care must be taken to follow the direction of signal flow. If there is a source (voltage clamp or current injection) at point *i* then the voltage gains A_{ij}, A_{jk}, and A_{jl} are meaningful because they follow the causal direction of signal flow, whereas A_{ji} is not, because it applies when a source at point *j* is producing a voltage at point *i*.

Rule 2: input admittance This rule also applies to the situation in Fig. 8, except the goal is to compute the input admittance $Y_{in} = \bar{I}_0 / \bar{V}_0$ at one end of a cylinder loaded with admittance Y_L at the other end. The calculation is done directly from Eqn. 38, evaluated at χ=0:

$$\begin{bmatrix} \bar{V}_0 \\ \bar{I}_0 \end{bmatrix} = \begin{bmatrix} \bar{V}(0,q) \\ \bar{I}_i(0,q) \end{bmatrix} = \begin{bmatrix} \cosh qL & \sinh qL/G_\infty q \\ G_\infty\, q \sinh qL & \cosh qL \end{bmatrix} \begin{bmatrix} \bar{V}_1 \\ Y_L\, \bar{V}_1 \end{bmatrix} \tag{41}$$

The input admittance is then the ratio of the two equations in Eqn. 41:

$$Y_{in} = \frac{\bar{I}_0}{\bar{V}_0} = G_\infty\, q \frac{\sinh qL + \dfrac{Y_L}{G_\infty q}\cosh qL}{\cosh qL + \dfrac{Y_L}{G_\infty q}\sinh qL} = G_\infty\, q \frac{\tanh qL + \dfrac{Y_L}{G_\infty q}}{1 + \dfrac{Y_L}{G_\infty q}\tanh qL} \tag{42}$$

A special case of importance is when Y_L=0, which is usually assumed at the end of a dendritic tree. In this case,

$$Y_{in} = G_\infty q \tanh qL \tag{43}$$

The second rule allows computation of the input admittance of any point on a dendritic tree. The computation is done constructively, as illustrated in Fig. 11. Consider the problem of

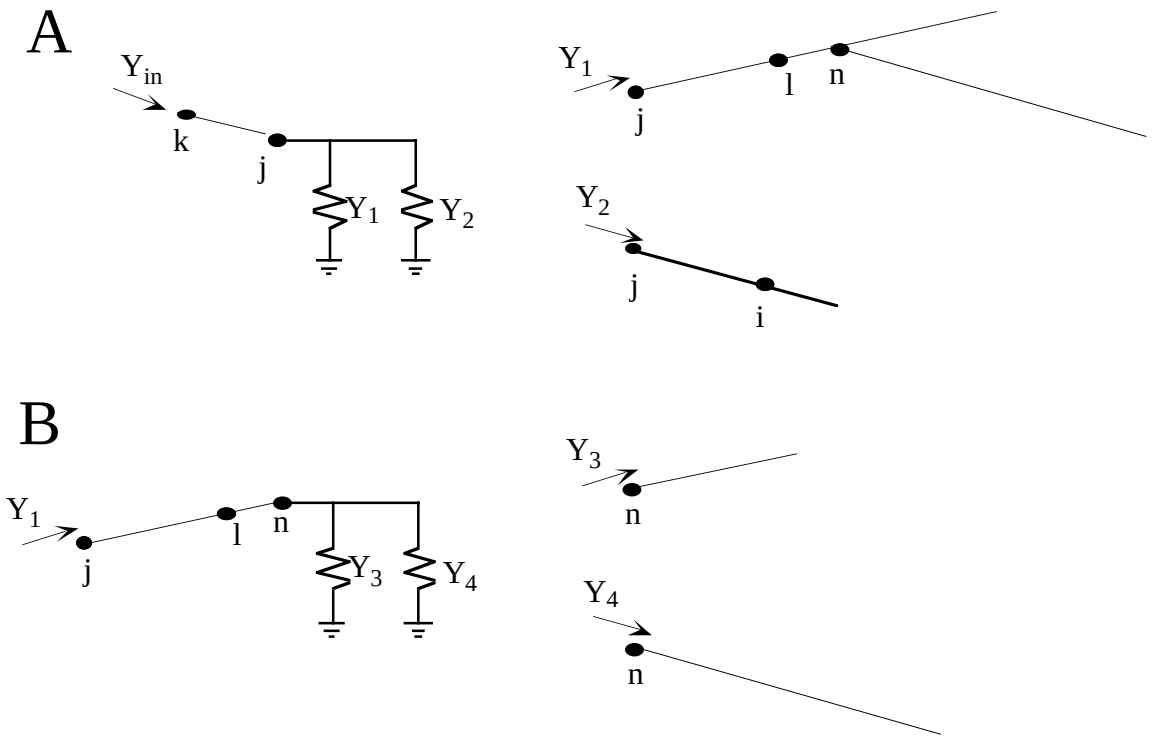

Figure 11 Illustrates the decomposition of the dendritic tree of Figure 10 in order to compute the input admittance at point *k*, looking out toward the end of the tree. A First segment of the tree, from *k* to *j*, terminated by input admittances of the two branches connected to *j*, shown at right. B Second segment, computing Y_1, the input admittance at *j* looking out the branch toward *l* and *n*.

computing the input admittance, looking out toward the end of the dendrites, at point *k* on the dendritic tree of Fig. 10. As shown in Fig. 11A, this is the input admittance of the cable from *k* to *j* terminated by the parallel combination of admittances Y_1 and Y_2. These are the input admittances of the two branches at *j*, shown at right in Fig. 11A. Admittance Y_2 can be computed immediately from Eqn. 43, because it is the input admittance of a single cable terminated at the end of the tree. Admittance Y_1 requires another decomposition, shown in Fig. 11B. At point *n* there are two branches, with input admittances Y_3 and Y_4. Both of these can be computed immediately from Eqn. 43. Once Y_3 and Y_4 are computed, Y_1 can be computed from Eqn. 42 using Y_3+Y_4 as the load admittance for the cable shown in the left part of Fig. 11B. Now the input admittance at *k* can be computed from Y_1 and Y_2 using Eqn. 42 and the cable in the left part of Fig. 11A.

Note that the input admittance at a point on the tree can be computed using this rule, by summing the input admittances looking away from the point in the two directions, toward and away from the soma.

Rule 3: transfer impedance The third rule allows calculation of the potential produced at a point by current injected at a different point. The situation is diagrammed in Fig. 12. A current $\bar{I}_{inj}$

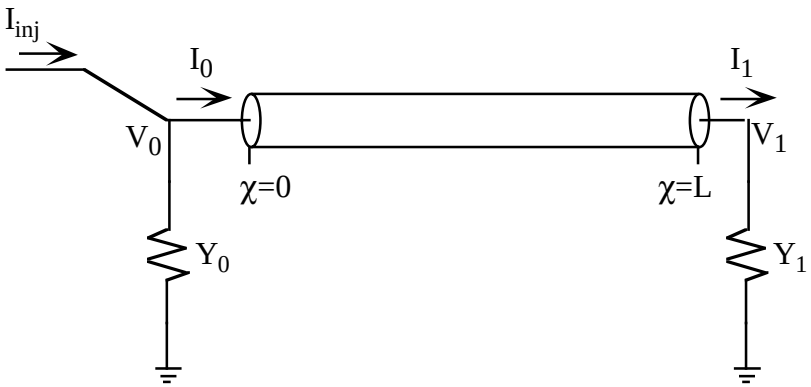

Figure 12 Cable terminated at both ends by admittances and driven at one end by an injected current.

is injected at one end of a cylinder and a potential $\bar{V}_1$ is produced at the other end. The relationship between these two can be computed by starting with Eqn. 35, evaluated at χ=L. With the constraints provided by the load impedance at the right end and the current injection at the left end, the equation gives

$$\begin{bmatrix} \bar{V}_1 \\ Y_1 \bar{V}_1 \end{bmatrix} = \begin{bmatrix} \cosh(qL) & -\sinh(qL)/G_\infty q \\ -G_\infty q \sinh(qL) & \cosh(qL) \end{bmatrix} \begin{bmatrix} (\bar{I}_{inj} - \bar{I}_0)/Y_0 \\ \bar{I}_0 \end{bmatrix} \tag{44}$$

If $\bar{I}_0$ is eliminated between the two equations in Eqn. 44, that leaves an equation relating $\bar{I}_{inj}$ and $\bar{V}_1$. The transfer impedance K_{01} is the ratio of these two quantities and is given by

$$K_{01} = \frac{\bar{V}_1}{\bar{I}_{inj}} = \frac{1}{(Y_0 + Y_1)\cosh qL + \left(\frac{Y_0 Y_1}{G_\infty q} + G_\infty q\right)\sinh qL} \tag{45}$$

The combination of transfer impedance and voltage transfer ratio can be used to compute transfer impedances between any two points in a dendritic tree. For example, for the tree in Fig. 10, if a current is injected at point *i*, the voltages at various other points on the tree will be given by Equations 46. Note how the branch points are handled. The transfer impedance K_{ij} cannot extend across a branch point, so the transfer impedance and voltage gain must be applied sequentially from branch point to branch point.

$$\begin{aligned} \bar{V}_j &= K_{ij}\,\bar{I}_{inj} & \bar{V}_k &= K_{ij}\,A_{jk}\,\bar{I}_{inj} \\ \bar{V}_l &= K_{ij}\,A_{jl}\,\bar{I}_{inj} & \bar{V}_n &= K_{ij}\,A_{jl}\,A_{ln}\,\bar{I}_{inj} \end{aligned} \qquad (46)$$

These relationships use Rules 1 and 3 explicitly; they also require Rule 2, however, in order to compute the admittances necessary to the use of Rules 1 and 3.

Question 6. Show that the following properties of the transfer impedance hold.

1. Symmetry: $K_{ij} = K_{ji}$

2. Positivity: $K_{ij} \le K_{ii}$ and $K_{ij} \le K_{jj}$ (for D.C. steady state (q=1 and all quantities real) only. The quantities K_{ii} and K_{jj} are the input impedances (resistances in the D.C. steady state) of the dendritic tree at points *i* and *j*.

3. Transitivity: $K_{ij} = K_{il}\,K_{lj}\,/K_{ll}$ True for points *i*, *l*, and *j* on a path without loops and point *l* in between *i* and *j*.

Question 7. Consider the Rall type model shown in Fig. 13. A current $\bar{I}_{inj}$ is injected at an electrotonic length L_1 from the soma. Compute the potential in the soma from the transfer impedance from L_1 to the soma.

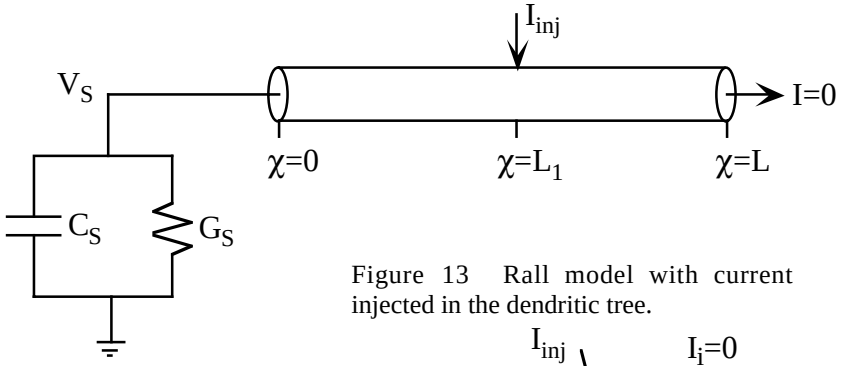

Figure 13 Rall model with current injected in the dendritic tree.

Question 8. A D.C. current I_{inj} is injected into a dendrite of the tree drawn in Fig. 14. Plot the potential distribution in all the dendritic branches. (Warning: this solution is very messy)

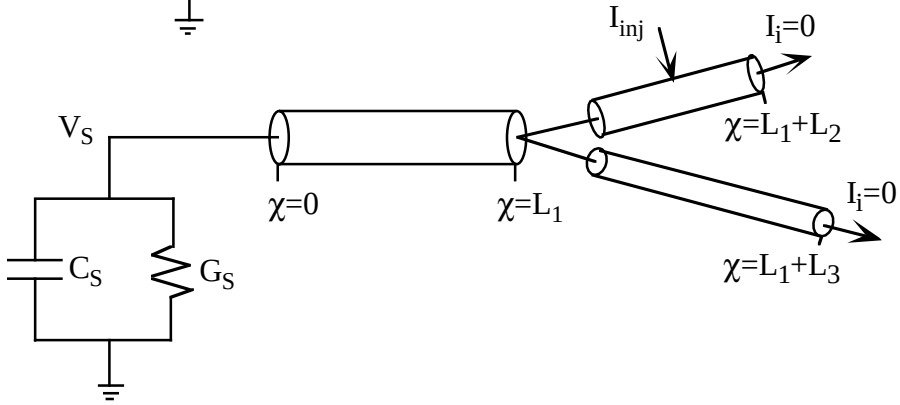

Figure 14: Rall-type model with a branched dendritic tree.

Question 9 Equations for the voltage gain and transfer impedance between points in a dendritic tree were derived above. It is also possible to imagine a current gain and a transfer admittance. The first is the ratio between the current injected into a cylinder and a current somewhere else in the dendritic tree. The second is the ratio between the voltage at one point in the tree and a current somewhere else. Construct reasonable definitions for the current gain and transfer admittance and write equations for them (Hint: these should follow directly from the results described above).

Equivalent cylinder theorem

The methods described in the previous section can be used to analyze linear cable problems of arbitrary complexity. In many cases, however, it is not necessary to have a detailed solution for currents and voltages in the dendritic tree. For example, in cases where the transfer function from a synapse on the dendritic tree to the soma is the matter of concern, it may be sufficient to approximate the dendritic tree with a single cylinder. The conditions under which this is possible are described in the following theorem, first studied by Rall (1962b).

Equivalent cylinder theorem. Consider an arbitrarily branching structure like the tree shown in Fig. 15. Three conditions can be stated:

1. The cumulative electrotonic lengths from soma to the tip of the dendritic tree is the same by all direct paths. That is, for the example in Fig. 15

$$L_{total} = L_{11} + L_{21} + L_{31} = L_{11} + L_{21} + L_{32} = \cdots = L_{11} + L_{22} + L_{34} \tag{47}$$

2. At every branch point, there is an impedance match in the sense that the sum of the G_∞s of the child branches equals the G_∞ of the parent branch. For example

$$G_{\infty 11} = G_{\infty 21} + G_{\infty 22} \quad \text{and} \quad G_{\infty 21} = G_{\infty 31} + G_{\infty 32} \quad \text{etc.} \tag{48}$$

   Note that this is usually stated as the 3/2 power law: at every branch point

$$a_{parent}^{3/2} = \sum_{\substack{\text{all child} \\ \text{branches } j}} a_j^{3/2} \tag{49}$$

3. The termination condition is the same at all dendritic tips, in the sense that $Y_{ij} / qG_{\infty ij}$ is the same for all terminal branches.

If these conditions are true, then the dendritic tree is equivalent to a cylinder with the electrotonic length L_{total}, a G_∞ value equal to $G_{\infty 11}$, and terminated by an admittance which is the sum of the admittances terminating the original tree. The equivalence holds in the following ways:

1. If the soma is voltage (or current) clamped, then $v(\chi)$ is the same in the original tree and the equivalent cylinder. Note that this rule applies to voltage measured in terms of electrotonic distance χ, not physical distance x.

2. The input admittance of the original tree is the same as that of the equivalent cylinder.

3. If current I_{inj} is injected into one branch at an electrotonic length L_I from the soma in the original tree, then the potential distribution is the same in the original tree and cylinder for the ultimate parent branch only. For example, if current were injected into branch *21* or *33* in the tree in Fig. 15, then the potential would be the same in the *11* branch and in the first L_{11} of the equivalent cylinder.

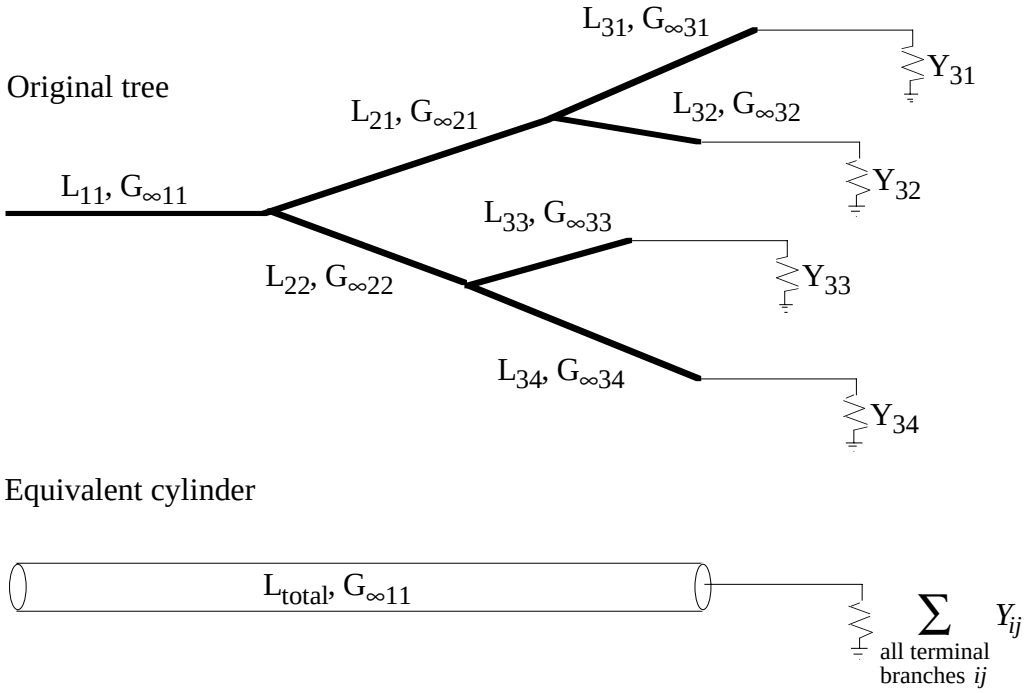

Figure 15 Top shows the branching structure of a dendritic tree with arbitrary termination admittances. Bottom shows the equivalent cylinder for this tree. *L* is electrotonic length equal to physical length divided by length constant. *G* is the infinite cylinder input conductance, Eqn. 13. *Y* is the admittance terminating each dendritic branch.

The proof of this theorem is straightforward, but algebraically messy. It can be done by proving each part for a single branch point (e.g. for parts *21*, *31*, and *32* of the tree in Fig. 15) and then extending the result to the whole tree by an induction-like process. The proofs can be easily done using the three rules in the previous section.

The premises of the equivalent cylinder theorem have been put to experimental test in a few neurons. These results will be described in class. The second premise of the theorem (Eqn. 48) is found to be true to good approximation. The third premise (equal termination admittances) has not been tested, and rests on the assumption of zero axial current flow at the end of the dendritic tree. The first premise (Eqn. 47) is not satisfied. What is found in real neurons is that the electrotonic

length from soma to dendritic tip varies considerably across branches. As a result of the failure of the first premise, real neurons are actually equivalent to cylinders whose radius is fixed near the soma, but gradually taper to zero radius farther from the soma.

Question 10 If the radius of the *11* branch in Fig. 15 is *a* cm and the lengths of the branches are l_{ij} cm write equations for the radius of the equivalent cylinder and its physical length.

Synapses are non-linear

An accurate model for the current injected into a membrane cable by a synapse is shown in Fig. 16. The synapse changes the conductance of the membrane through its own conductance change G_{syn}. The current flow into the cylinder is

$$\bar{I}_{syn} = G_{syn}(E_{syn} - \bar{V}) \qquad (50)$$

where $\bar{V}$ is the membrane potential of the cylinder at the location of the synapse. The nonlinearity of this equation comes from the fact that $\bar{V}$ changes with the synaptic current:

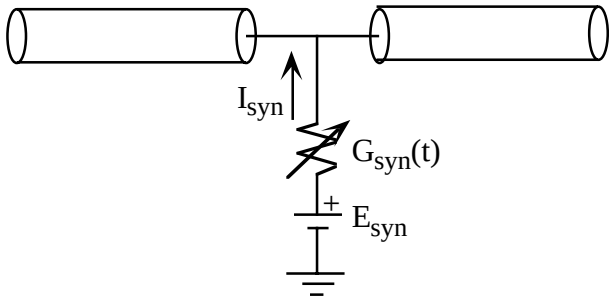

Figure 16 Model for the current flow into a cylinder due to a synaptic conductance change.

$$\bar{V} = K_{ss}\bar{I}_{syn} \quad \text{so} \quad \bar{I}_{syn} = \frac{G_{syn}E_{syn}}{1 + G_{syn}K_{ss}} \qquad (51)$$

where K_{ss} is the input impedance of the cylinder at the point of the synapse. This can be computed from Rule 2 in the previous section. The right hand part of Eqn. 51 shows that the injected current is related to the synaptic input conductance in a nonlinear fashion. Matters become worse when the interaction of two synapses is considered. Suppose there is a second synapse nearby. When the second synapse is activated, K_{ss} in Eqn. 51 will change because of the effects of the second synapse's conductance change. The the activation of a synapse changes the current injected by all nearby synapses, producing nonlinear summation of synaptic inputs.

Nonlinear interactions in dendritic trees cannot be analyzed with the analytical methods developed in these notes. Instead, simulation of approximations to dendritic trees are used. In these methods, the dendritic tree is broken up into compartments, like those in Fig. 1, and equations like Eqns. 1, 3, and 4 are written and solved by simulation. This method was developed by Rall in a seminal paper in 1964. The membane currents are represented by full Hodgkin-Huxley type models, allowing the incorporation of voltage and calcium dependent conductances into the model. For a discussion of these methods, see Koch and Segev (1998), Chapters 3 and 5.

References

Hodgkin, A.L. and Rushton, W.A.H. The electrical constants of a crustacean nerve fibre. *Proc. Roy. Soc.* B-133, 444-79 (1946).

Jack, J.J.B. , Noble, D., and Tsien, R.W. *Electric current flow in excitable cells*. Clarendon Press, Oxford (1975).

Johnston, D. and Wu, S.M. Foundations of Cellular Neurophysiology. MIT Press, Cambridge (1995).

Koch, C. *Biophysics of Computation*. Oxford Press, New York (1999).

Koch, C. and Segev, I. *Methods in Neuronal Modeling from Ions to Networks* (2nd Ed.). MIT Press, Cambridge (1998).

Rall, W. Theory and physiological properties of dendrites. *Ann. N.Y. Acad. Sci.* 96:1071-1092 (1962a).

Rall, W. Electrophysiology of a dendritic neuron model. *Bioph. J.* 2:145-67 (1962b).

Rall, W. Theoretical significance of dendritic trees for neuronal input-output relations. In *Neural Theory and Modeling*, R.F. Reiss (Ed.). Stanford Univ. Press, Palo Alto. Reprinted in *The Theoretical Foundation of Dendritic Function*, I. Segev, J. Rinzel, and G.M. Shepherd (Eds.) MIT Press, Cambridge (1995).

Rall, W. Time constants and electrotonic length of membrane cylinders and neurons. *Bioph. J.* 9:1483-1508 (1969).